ARTICLE

OBC
www.rsc.org/obc

The influence of hydrogen bonding interactions on the C–H bond activation step in class I ribonucleotide reductases †

Hendrik Zipse*
Department Chemie, LMU München, Butenandtstr. 13, D-81377 München, Germany

Received 25th October 2002, Accepted 13th December 2002
First published as an Advance Article on the web 22nd January 2003

In order to model the C–H bond activation step in ribonucleotide reductases the hydrogen atom abstraction reaction from *cis*-tetrahydrofuran-2,3-diol (**7**) by methylthiyl (**8**) radical has been studied with theoretical methods. In order to identify an appropriate theoretical method for this system, the hydrogen transfer reaction between radical **8** and methanol (**9**) to give methanol radical (**10**) and methyl thiol (**11**) has been studied at several different levels of theory. While the reaction energy for this process is predicted equally well by the Becke3LYP and BHandHLYP hybrid functional methods, the reaction barrier is predicted to be significantly lower by the former. Compared to results obtained at CCSD(T)/cc-pVTZ level the BHandHLYP functional is better suited for the calculation of activation barriers for hydrogen abstraction reactions. This latter method was subsequently used to study the reaction of radical **8** with *cis*-tetrahydrofuran-2,3-diol **7** in the absence and in the presence of additional functional groups (acetate and acetamide) as models for the substrate reaction of class I ribonucleotide reductases (RNRs). The reaction barrier is lowest in those systems, in which acetate forms a double hydrogen bonded complex with the hydroxy groups of diol **7** (+8.2 kcal mol^{-1}) and increases somewhat for side-on complexes between substrate **7** and acetate featuring only one hydrogen bond (+10.5 kcal mol^{-1}). The barrier reduction of 6.5 kcal mol^{-1} obtained through complexation of diol **7** with acetate appears to be due to the formation of short strong hydrogen bonds in the transition. These effects can also be found in reactions of thiyl radical **8** with complexes of diol **7** with acetamide, but to a much smaller extent. The lowest reaction barrier is in this case calculated for the side-on complex (+11.2 kcal mol^{-1}), while the bridging orientation between diol **7** and acetamide leads to a reaction barrier (+13.4) that is only slightly lower than that for the uncatalyzed process (+14.7 kcal mol^{-1}). With respect to the structure of the active site of the RNR R1 subunit, only the side-on complexes appear to be relevant for the enzyme-catalyzed process. Under this condition the influence of the E441 side chain and thus the impact of the E441Q mutation in the initial C–H bond activation step will be rather small.

Introduction

Ribonucleotide reductases (RNRs) catalyze the reduction of nucleotides to 2′-deoxynucleotides.[1] In class I RNRs the actual reduction step is performed in the R1 subunit after hydrogen atom transfer has occurred to a radical source in the R2 subunit. Scheme 1 shows a minimal representation of the proposed reaction mechanism of the reduction process.[1] This sequence involves, after generation of a sulfur centered radical at cystein C439, abstraction of a hydrogen atom from the C3′ position of the bound substrate. Radical **2** generated in this first step through hydrogen abstraction from substrate **1** then loses one molecule of water, forming α-keto radical **3**. Subsequent hydrogen atom transfer from the adjacent C462/C225 thiol groups leads to formation of ketone **4**. A combination of electron transfer from the disulfide radical anion present in the active site and proton transfer from the protonated E441 carboxylate group gives C3′-radical **5**. The ultimate step in the reaction sequence is hydrogen atom transfer from the C439 thiol group, forming the closed shell reduction product **6** and regenerating the sulfur centered radical. It is obvious from this sequence that C439 is essential for initiation of the reduction sequence and that the presence of C462 and C225 is required for the actual reduction process in steps 2–4.[2] The role of glutamate E441 in the reduction process is, however, less clear. The X-ray structure of the R1 subunit by Eriksson *et al.* shows the E441 carboxylate group to be positioned in close vicinity to the substrate C2′ and C3′ carbon atoms.[3] It has been suggested that the carboxylate group of E441 functions as a general base for water elimination in the second step of the overall reaction mechanism,[1] in line with previous results obtained in model studies for this process.[4,5] That the presence of a carboxylate group will also lower the barrier for the initial C–H bond activation step has been the result of a recent theoretical study using ethylene glycol as a substrate model.[6] Using somewhat larger model systems, Siegbahn has provided theoretical evidence that the presence of E441 in its neutral state together with a neighboring amide group from asparagine N437 lowers the barrier for C–H bond activation somewhat, but dramatically reduces the barrier for the subsequent water elimination step.[7]

Experimental support for the involvement of E441 in the early steps of the RNR substrate mechanism includes biochemical studies with RNR mutants, in which glutamate E441 was replaced by glutamine (E441Q).[8,9] The spectroscopic results obtained using the E441Q mutants led Sjöberg *et al.* to suggest that the C–H bond activation step is slowed down considerably in the absence of the E441 carboxylate group and that the C439 thiyl radical as well as the subsequently formed substrate C3′ radical are thus detectable through rapid freeze EPR spectroscopy at 9 GHz.[8] Reinvestigating the substrate reaction of the same mutant with considerably better analytical techniques (140 GHz EPR spectroscopy) Stubbe *et al.* assigned the two signals observed before to a disulfide radical anion and a new substrate radical suggested to be of the C4′ ketyl type.[9] This reassignment implies that the effect of the E441 carboxylate group on the first two steps in the substrate mechanism is rather minor but that the presence of E441 in its neutral form is required for reduction of the C3′ ketone **4**. That the C4′ ketyl radical produced by the E441Q mutant represents a surprisingly stable intermediate not considered before and that the carboxylate group in its protonated form does indeed catalyze the reduction of intermediate **4** was confirmed in a recent

† Electronic supplementary information (ESI) available: Energies and structures of stationary points for studied reactions. See http://www.rsc.org/suppdata/ob/b2/b210536p/

DOI: 10.1039/b210536p

 This journal is © The Royal Society of Chemistry 2003

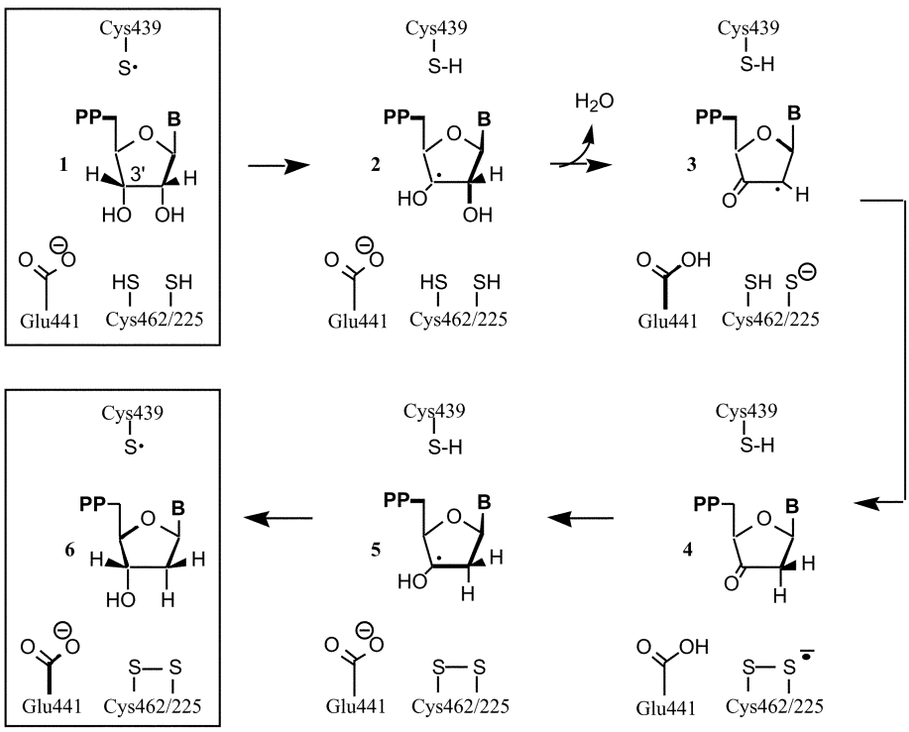

Scheme 1

Table 1 Reaction energies (0 K) and enthalpies (298 K) as well as activation energies (0 K) for the reaction of methylthiyl radical (**8**)[a] with methanol (**9**) to give methanol radical (**10**) and methyl thiol (**11**). All values are in kcal mol^{-1}

	8 + 9 ⟶ 10 + 11		**12 ⟶ 13**	**12 ⟶ 14**
Method	Δ*E*(0 K)	Δ*H*(298 K)	Δ*E*(0 K)	Δ*E*(0 K)
B3LYP/DZVP	+12.7	+12.9	+15.9	+11.5
B3LYP/LB//B3LYP/DZVP	+9.6	+9.8	+13.4	+8.4
B3LYP/LB	+9.5	+9.8	+13.5	+8.3
BHLYP/DZVP	+14.0	+14.2	+20.6	+12.9
BHLYP/LB//BHLYP/DZVP	+10.5	+10.7	+17.8	+9.5
BHLYP/LB	+10.4	+10.7	+17.9	+9.3
UCCSD(T)/cc-pVTZ//B3LYP/LB	+10.4	+10.7	+16.3	+9.0
G2[b]	+10.1	+10.3	—	—
Experiment[b]	—	+8.80 ± 1.5	—	—

[a] C_s-symmetry, A′ state. [b] Values from ref. 22.

theoretical study by Himo and Siegbahn[10] That still leaves us with the question, whether the glutamine side chain in the E441Q mutant has filled in for the wild type carboxylate group to some extent through hydrogen bonding to the C2′ and C3′ hydroxy groups. We therefore reinvestigate here the reaction of 2,3-dihydroxytetrahydrofuran **7** as a substrate model with methylthiyl radical **8** in the absence of any functional groups as well as the presence of acetate as a model for glutamate and acetamide as a model for glutamine. This choice of model systems also allows us to further probe the role of hydrogen bonding or partial proton transfer[11] in enzyme catalyzed radical reactions.

Theoretical methods

As in our earlier study,[6] all geometry optimizations were performed with the split valence double zeta basis set (DZP) optimized by Godbout *et al.*[12] using either the Becke3LYP[13] or the Becke-half-and-half-LYP (BHLYP)[14] hybrid density functional. All energy differences reported in this manuscript as "Δ*E*(0 K)" include the unscaled difference in zero point vibrational energies, while all enthalpy differences have been calculated using harmonic vibrational frequencies and a temperature of 298 K. Single point energies have also been calculated using the somewhat larger 6-311+G(2d,p) basis set which will be denoted as "LB". For the smallest model systems, single point calculations have also been performed at the UCCSD(T)/cc-pVTZ level. Relative energies calculated at this level have been combined with B3LYP/LB thermal corrections to give the energies listed in Tables 1 and 2. Cumulative partial charges have been obtained from a Mulliken population analysis using the DFT Kohn–Sham orbitals.[15] All calculations have been performed with *Gaussian 98*.[16]

Results

Selection of a theoretical method: the reaction of methanol with methylthiyl radical

Most previous quantum mechanical studies of some aspects of the RNR substrate mechanism have resorted to the Becke3LYP hybrid density functional method in combination with medium sized basis sets.[6,10,17] That this level of theory might not be an optimal choice for open shell species has been the result of recent theoretical studies on radical ions.[18–20] But also for neutral open shell systems, Becke3LYP calculations yield

Table 2 Relative energies/kcal mol^{-1} for stationary points in the reaction of methylthiyl radical (**8**) with tetrahydrofuran-2,3-diol (**7**)

	ΔE		ΔE	
Structure	[BHLYP/DZP]	[BHLYP/LB//BHLYP/DZP]	[B3LYP/DZP]	[B3LYP/LB//B3LYP/DZP]
7 + **8**	0.0	0.0	0.0	0.0
16	−1.57	−1.23	−0.92	−0.49
16b	−3.03	−3.09	−2.61	−2.79
17	+15.93	+13.41	+11.01	+8.54
17b	+17.05	+14.24	+12.88	+10.02
18	+10.56	+7.53	+9.03	+6.04
18b	+8.92	+5.64	+7.46	+4.00
11 + **15**	+11.81	+8.57	+9.84	+6.70

reaction barriers that are systematically too low.[21] This problem can, in part, be circumvented by increasing the amount of Hartree–Fock exchange contribution in the hybrid functional and the BeckeHandHLYP functional has given systematically better results in this respect.[18–21] In order to assess the influence of the density functional method on the calculated barrier heights for hydrogen transfer reactions, the reaction of methylthiyl radical **8** with methanol **9** has been studied at several different levels of theory.

The reaction of radical **8** with methanol has been studied before at the Becke3LYP/DZP level of theory.[6] These two species react to give methanol radical (**10**) and methyl thiol (**11**) (Scheme 2). The reaction energies (at 0 K) as well as the reaction

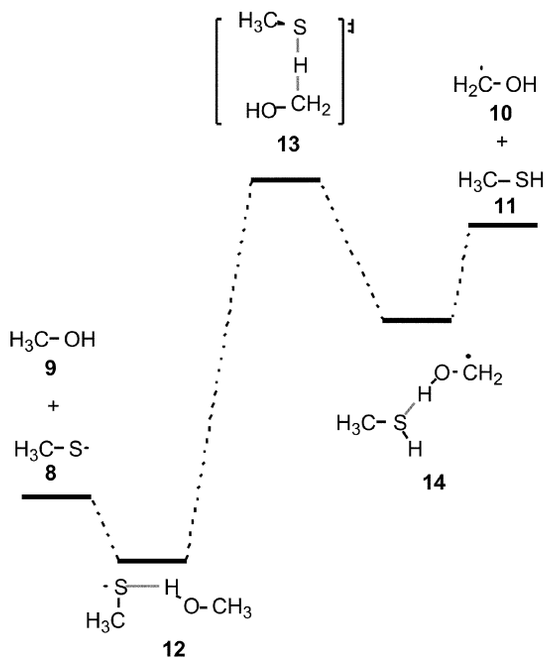

Scheme 2

enthalpies (at 298 K) calculated at various levels of theory have been collected in Table 1. All methods listed in Table 1 agree in that thermal corrections are very small for this reaction. Also, both the B3LYP[6] as well as the BHLYP functionals provide a significantly better prediction of the reaction enthalpy when using a larger basis set.

Comparison of the BHLYP/LB//BHLYP/DZP and the BHLYP/LB results shows that the combination of geometry optimization with a smaller basis set and single point energy calculations with the larger 6-311+G(2d,p) basis gives more or less the same result as compared to full optimization using the larger basis set. Reaction enthalpies calculated using the BHLYP functional are slightly more endothermic as compared to the B3LYP functional, regardless of the basis set used. While the BHLYP/LB results are very close to those obtained from UCCSD(T) single point or from G2 calculations, the B3LYP/LB results are closer to the experimental value. Given that the BHLYP and B3LYP results differ by less than 1 kcal mol^{-1}, it appears that the reaction energetics can be predicted equally well with both functionals.

The reaction barrier calculated as the energy difference between ground state complex **12** and transition state **13** depends more strongly on the chosen theoretical method. Using the UCCSD(T) value as the reference, the B3LYP/LB barrier is 2.8 kcal mol^{-1} too low, while the BHLYP/LB value is 1.6 kcal mol^{-1} too high. These differences are certainly not alarmingly large, but still suggest that use of the BHLYP hybrid functional might be more appropriate for the current purpose. We will therefore concentrate on the BHLYP/LB results in the following.

The reaction of tetrahydrofuran-2,3-diol 7 with methylthiyl radical

The reaction of radical **8** with diol **7** defines the reference reaction for which the effects of hydrogen bonding through external functional groups will be studied. The potential energy surface calculated at the BHLYP/LB level of theory is actually quite similar to that obtained at B3LYP/LB level[6,7] (Scheme 3a and 3b).

The most favorable transition state for hydrogen abstraction **17** leads from ground state complex **16** to product complex **18**. In all these structures the pattern of hydrogen bonding is similar in that the hydroxy group attached to the reaction center (in the following termed the C3′ center) donates a hydrogen bond to the neighboring hydroxy group (the C2′ position). Neither the H–O distance of 2.24 Å nor the O–H–O angle of 106.4° is indicative of particularly strong hydrogen bonding (Fig. 1). Transition state **17** is located 13.4 kcal mol^{-1} above the separate reactants **7** and **8** and 14.6 kcal mol^{-1} above reactant complex **16**. The choice of a reference point is, however, by no means a trivial task as other reactant complexes at lower energy and with a different hydrogen bonding pattern exist. Particularly stable are complexes, in which the attacking sulfur radical forms a hydrogen bond with the C3′ hydroxy group such as **16b** (Scheme 3b). Despite its favorable energetics complex **16b** might not be involved in the enzyme catalyzed process for two reasons. First, according to the X-ray structure of the R1 subunit the Cys439 thiol group is not in contact with the substrate C3′ hydroxy group.[3] This can, of course, change through radical formation at Cys439 but would still require substantial reorientation of the bound substrate in the active site.

Second, the hydrogen bond formed in complex **16b** must be cleaved again *en route* to the corresponding transition state **17b** which is located 14.2 kcal mol^{-1} above the separated reactants **7** and **8**, or +17.3 kcal mol^{-1} above reactant complex **16b**, and is 0.8 kcal mol^{-1} less favorable than transition state **17**. This latter energy difference implies that the hydrogen bonding pattern in transition state **17** (C3′–OH as donor, C2′–OH as acceptor) is only slightly more favorable in energetic terms than the arrangement in **17b** (C3′–OH as acceptor, C2′–OH as donor). The similar energetics are also reflected in the comparable electronic structure of **17** and **17b**. In both structures the

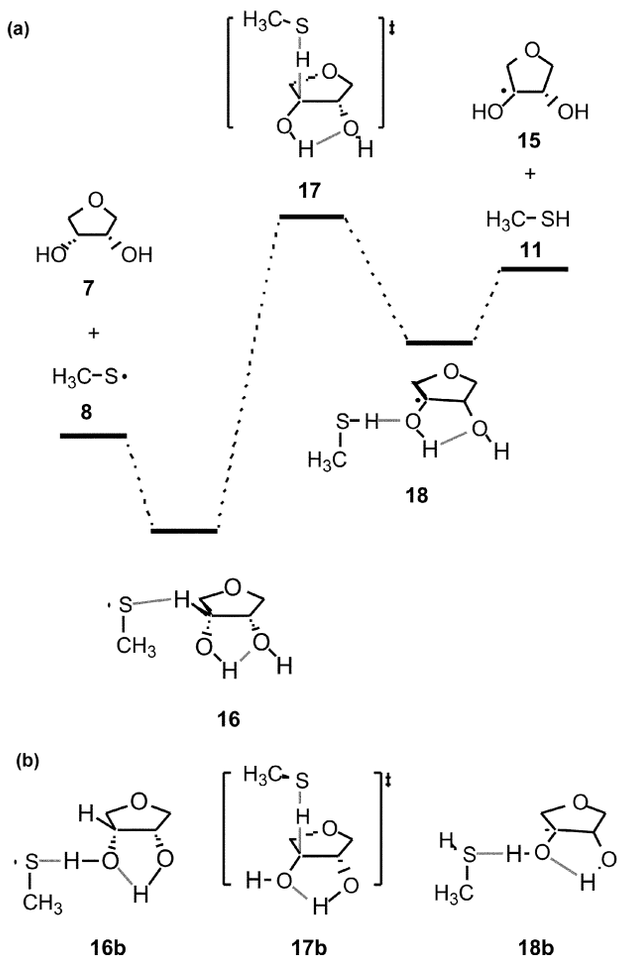

Scheme 3

cumulative charge over the CH3S and CH3SH fragments amounts to $-0.09e$ and $-0.10e$, respectively, and the unpaired spin density is distributed over the C3′ carbon atom (0.64) and the sulfur atom (0.39).

Since all stationary points shown in Schemes 3a and 3b are also available at the B3LYP level of theory,[6] a comparison of B3LYP and BHLYP reaction barriers can be made. Transition state **17** is predicted to lie +9.03 kcal mol^{-1} above reactant complex **16** at the B3LYP level and +14.6 kcal mol^{-1} at the BHLYP level. This amounts to a difference of 5.6 kcal mol^{-1}, significantly more than calculated for the smaller model system shown in Scheme 2. A similar conclusion can be reached comparing the activation barriers for transition state **17b**. These results indicate that the B3LYP/BHLYP barrier difference increases (rather than decreases) with lower reaction barriers. The very low barriers found in previous theoretical studies for some steps in the RNR mechanism at the B3LYP level might therefore not be too realistic.

Reaction of tetrahydrofuran-2,3-diol 7 with methylthiyl radical in the presence of acetate

Several transition states for the reaction of radical **8** with acetate complex **19** can be envisaged based on their hydrogen bonding patterns: (a) systems in which acetate coordinates to both diol hydroxy groups, and (b) systems in which acetate coordinates only to the C3′ hydroxy group. The most favorable transition state **22a** belongs to the first group (Scheme 4). The relative orientation between acetate and the furan ring system can best be described as "front side" as is clearly visible in the structure of **22a** (Fig. 1). The significantly higher complexation energy between substrate complex **19** and methylthiyl radical **8** of

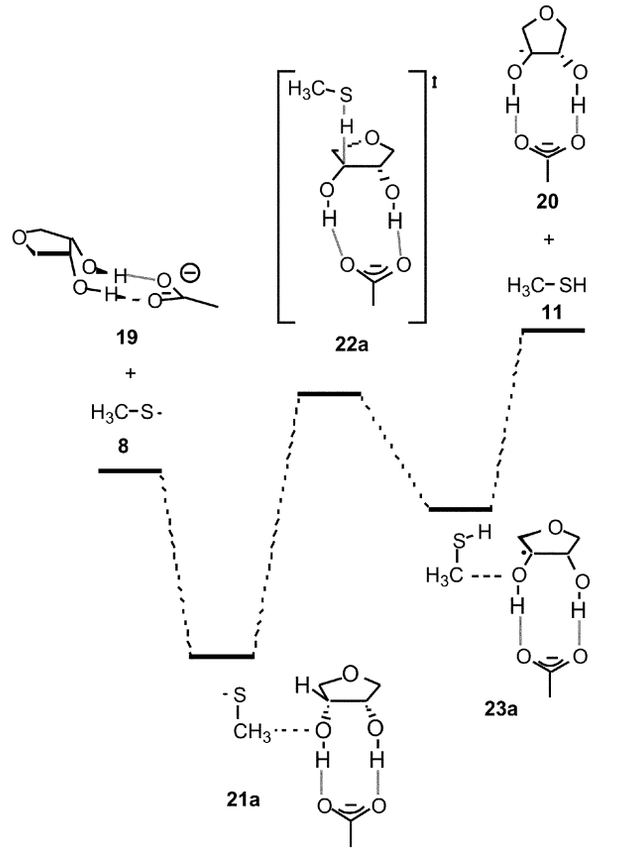

Scheme 4

−5.9 kcal mol^{-1} as compared to that between **7** and **8** is not due to formation of additional hydrogen bonds, but to unspecific ion-dipole interactions (Table 3). Due to this higher complexation energy, transition state **22a** is located 8.2 kcal mol^{-1} above reactant complex **21a**, but only 2.3 kcal mol^{-1} above the separate reactants **8** and **19**. The product complex **23a** formed after passing through **22a** differs from **18** in that no hydrogen bond is formed between methyl thiol and the acetate group. The reaction endothermicity calculated for the separate reactants and products of +4.3 kcal mol^{-1} is therefore very similar to that calculated for the reactant and product complexes of +4.6 kcal mol^{-1}. Compared to the parent system lacking the acetate group, this represents a reduction of the reaction endothermicity by 4.2 kcal mol^{-1}. The intracomplex reaction barrier (calculated as the energy difference between transition state and the preceding reactant complex) is also lowered from +14.6 kcal mol^{-1} in the parent system to +8.2 kcal mol^{-1} after acetate complexation.

This barrier lowering is accompanied by transfer of some of the negative charge to the methylthiyl radical in transition state **22a**, which carries an overall negative charge of $-0.20e$. An interesting geometrical feature of transition state **22a** is the length of the carboxylate hydrogen bond to the C3′ hydroxy group which is significantly shorter at 1.59 Å as compared to the hydrogen bond to the C2′ hydroxy group at 1.74 Å. This difference in hydrogen bond distances is much smaller in ground state complex **21a**, in which the hydrogen bond distances to the C3′ and C2′ hydroxy groups amount to 1.72 and 1.77 Å, respectively. In product complex **23a**, in which the C3′ position has turned into a radical center known to enhance the acidity of α-hydroxy groups substantially,[4] the two hydrogen bond distances to the C3′ and C2′ hydroxy groups are slightly longer than in the transition state at 1.62 and 1.76 Å, respectively. If the hydrogen bond distances are reflective of the acidity of a given hydroxy group one must conclude that transition state **22a** is the most acidic structure along the reaction pathway for hydrogen atom abstraction at the C3′ position. That the

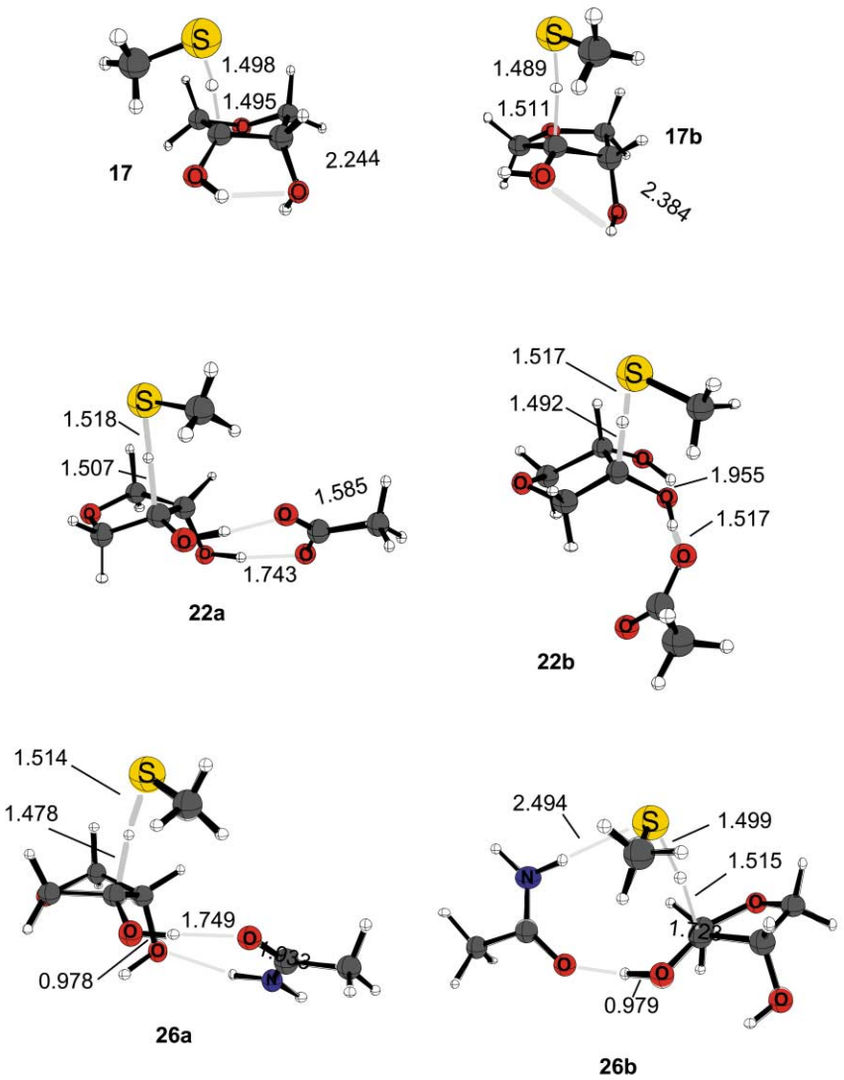

Fig. 1 Structures of transition states **17**, **22**, and **26** (BHLYP/DZP).

Table 3 Relative energies/kcal mol^{-1} for stationary points in the reaction of methylthiyl radical (**8**) with tetrahydrofuran-2,3-diol (**7**) in the presence of acetate and acetamide

	ΔE			ΔE	
Structure	[BHLYP/DZP]	[BHLYP/LB//BHLYP/DZP]	Structure	[BHLYP/DZP]	[BHLYP/LB//BHLYP/DZP]
8 + **19**	0.0	0.0	**8** + **24**	0.0	0.0
21a	−6.18	−5.87	**25a**	−1.85	−1.61
21b	−2.77	−2.53	**25b**	−0.21	+0.04
22a	+4.93	+2.33	**26a**	+14.39	+11.80
22b	+11.13	+7.99	**26b**	+14.29	+11.25
23a	+1.88	−1.24	**27a**	+8.55	+5.17
23b	+8.34	+4.91	**27b**	+10.80	+7.39
11 + **22**	+8.06	+4.33	**28** + **11**	+10.48	+6.87

drop in reaction barrier of 6.4 kcal mol^{-1} is actually significantly larger than the drop in reaction energy can be taken as an indication for the truly catalytic activity of the acetate group. This has also been found for formate as a catalyst in our previous study using simpler model substrates.[6] Alternative conformations of doubly hydrogen bonded complex **21a** exist which are energetically less favorable and will therefore not be discussed here any further.

The most favorable transition state from group (b) featuring only one hydrogen bond between acetate and diol substrate **7** is **22b** (Scheme 5). In this case the acetate is oriented such that the non-coordinating acetate oxygen atom is pointing away from the attacking methylthiyl radical (Fig. 1). This orientation is maintained all along the reaction pathway starting at reactant complex **21b** and ending at product complex **23b**. However, the length of the connecting hydrogen bond varies dramatically in that ground state complex **21b** is characterized by a "long" hydrogen bond of 1.64 Å, while much shorter bond distances are found in transition state **22b** and product complex **23b** with 1.42 Å and 1.50 Å, respectively. That the hydrogen bond is shortest in transition state **22b** again suggests that this is the most acidic structure along the pathway. The intracomplex activation barrier for this pathway is +10.5 kcal mol^{-1}, approximately 2 kcal mol^{-1} more than for transition state **22a**. Despite these differences the reaction barriers are in both cases lower than those calculated for the parent system lacking the acetate group. The overall charge of the methylthiyl radical in **22b** is −0.20*e*, identical to that in transition state **22a**. Again,

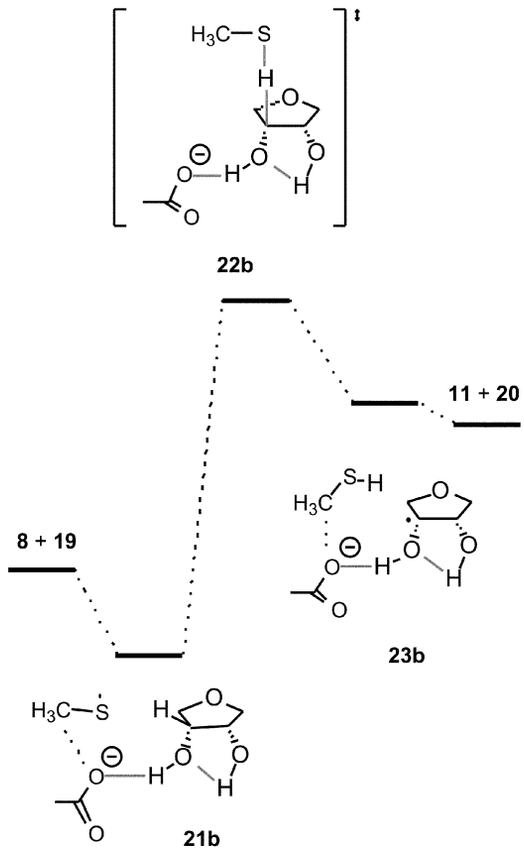

Scheme 5

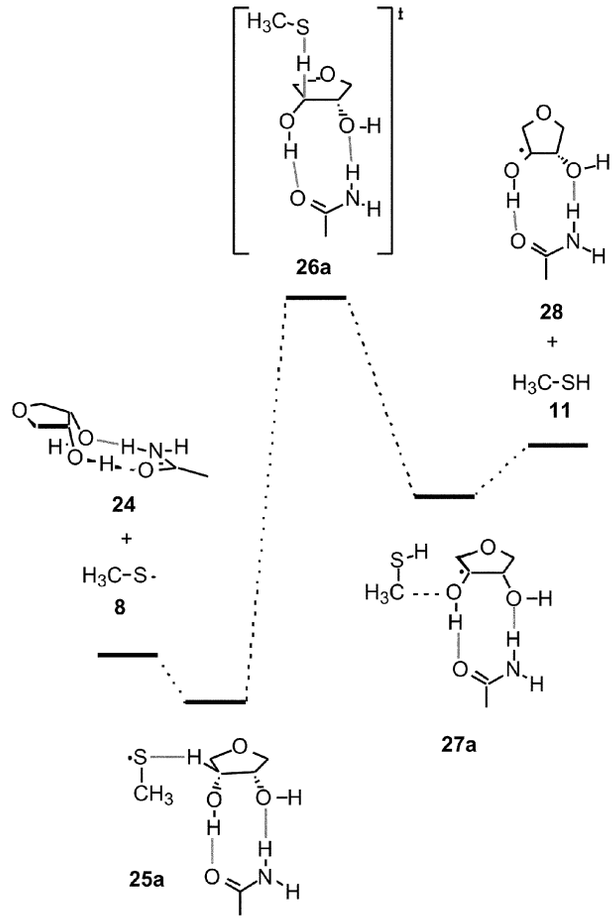

Scheme 6

other conformations of transition state **22b** and ground state complex **21b** exist at slightly higher energies with similar orientations between the acetate group and the dihydrofuran substrate.

The reaction of tetrahydrofuran-2,3-diol 7 with methylthiyl radical in the presence of acetamide

Transition states for the reaction of thiyl radical **8** with complexes of diol **7** with acetamide are similarly numerous as found before for acetate complex **19**. In keeping with the division into bridged and side-on complexes we will first discuss those transition states in which both hydroxy groups of substrate **7** participate in hydrogen bonding with the acetamide "catalyst". The energetically most favorable reaction pathway leads through transition state **26a**, located 10.2 kcal mol^{-1} over reactant complex **25a** (Scheme 6).

This latter complex is formed from substrate complex **24** through weak and unspecific association with radical **8**. The mode of coordination between diol substrate and acetamide in **26a** is maintained throughout the reaction pathway that ultimately ends at product complex **28** and thiol **11**. The reaction energy is significantly endothermic at +6.9 kcal mol^{-1}, which has to be compared to the endothermicity of the uncatalyzed and the acetate-catalyzed systems at +8.6 and +4.3 kcal mol^{-1}, respectively. The largest structural difference between transition state **26a** and the corresponding transition state in the acetate series **22a** can be found in the hydrogen bonds formed between substrate and catalyst (Fig. 1). While both hydroxy groups act as hydrogen bond donors in **22a**, the C3′ hydroxy group in **26a** acts as hydrogen bond donor and the C2′ hydroxy group acts as H-bond acceptor. The characteristic variation of the hydrogen bond length to the C3′ hydroxy group observed for the acetate system is much reduced now in the presence of acetamide with bond distances of 1.84, 1.75, and 1.75 Å for ground state **25a**, transition state **26a** and product complex **27a**, respectively. The cumulative charge of the methylthiyl radical in **26a** is slightly negative at −0.11*e*. Both factors, the reduced amount of charge transfer to the methylthiyl radical as well as the smaller variation of hydrogen bond distances along the reaction pathway suggest that acetamide will be a less effective catalyst for the hydrogen abstraction reaction at C3′. Other variations in the series of bridged transition states include a "bottom side" complexation mode as well as those, in which the C2′ (and not the C3′) hydroxy group donates a hydrogen bond to acetamide, while the C3′ hydroxy group accepts a hydrogen bond from the acetamide amine terminus. All of these are less favorable than transition state **26a** by at least 3 kcal mol^{-1} and will therefore not be considered here.

The most favorable transition state for a "side-on" complex between substrate diol **7** and acetamide is **26b** (Fig. 1). This structure features a hydrogen bond between the C3′ hydroxy group and the acetamide oxygen atom while the C2′ hydroxy group forms an internal (but weak) hydrogen bond to the C3′ hydroxy group. Acetamide is oriented such that it donates an additional hydrogen bond to the sulfur atom of the attacking thiyl radical. This hydrogen bond, though rather large in **26b** at 2.48 Å, might help to stabilize the small partial negative charge of −0.12*e* that develops on the methylthiyl radical in transition state **26b**. Variation of the hydrogen bond distance to the C3′ hydroxy group is somewhat more visible in this system with values of 1.82, 1.71, and 1.73 for ground state complex **25b**, transition state **26b**, and product complex **27b**, respectively.

The reaction pathway through **26b** starts at reactant complex **25b** (Scheme 7), located 0.1 kcal mol^{-1} above the separated reactants **8** and **24**. The bridged substrate complex **24** has been chosen here as the reference in order to provide a common point of reference to the reaction pathways shown in Schemes 6 and 7. After passing through **26b** the product complex **27b** is formed. This latter structure is located 7.4 kcal mol^{-1} above the ground state complex **25b**. Transition states with a different

Table 4 Reaction barriers $\Delta E_C^{\ddagger}$, reaction energies $\Delta E_{C,RXN}$, and intrinsic reaction barriers $\Delta E_{C,0}^{\ddagger}$ Calculated from eqn. (1) for the most favorable reaction pathways for C–H bond activation in diol **7**. Values for a local and a global reference are given (in kcal mol^{-1})

	Local reference			Global reference	
Transition state	$\Delta E_C^{\ddagger}$	$\Delta E_{C,RXN}$	$\Delta E_{C,0}^{\ddagger}$	$\Delta E_C^{\ddagger}$	$\Delta E_{C,RXN}$
No catalyst					
17	+14.7	+8.8	+9.8	+16.5	+8.7
Acetate as catalyst					
22a (bridged)	+8.2	+4.6	+5.7	+8.2	+4.6
22b (side on)	+10.5	+7.0	+6.6	+13.9	+4.6
Acetamide as catalyst					
26a (bridged)	+13.4	+6.8	+9.7	+13.4	+6.8
26b (side on)	+11.2	+7.4	+7.1	+12.9	+6.8

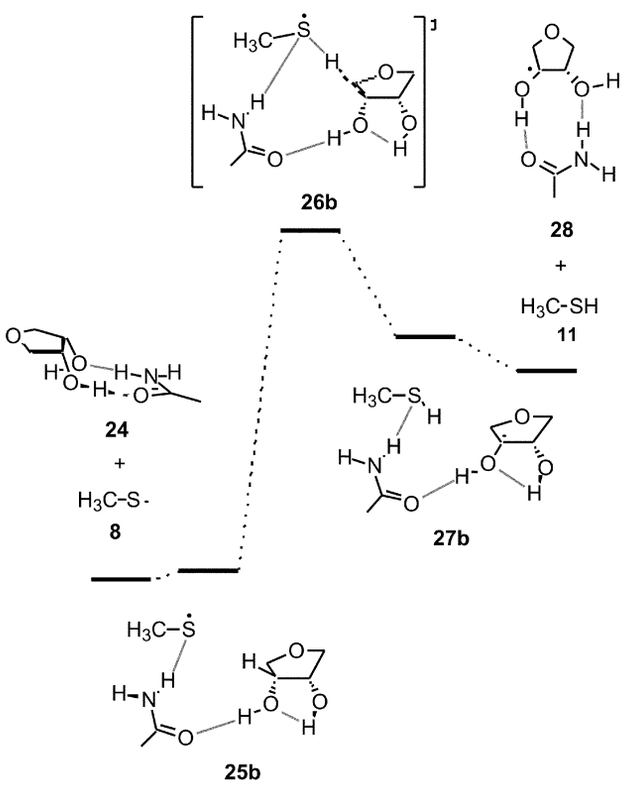

Scheme 7

conformation of the tetrahydrofuran ring but a comparable orientation of thiyl radical and acetamide as in **26b** exists at slightly higher energies and will not be discussed here any further.

Discussion

For the sake of comparing the activation barriers for hydrogen atom abstraction from *cis*-tetrahydrofuran-2,3-diol **7** in the absence as well as the presence of additional functional groups all reaction barriers have been collected in Table 4. The activation barriers are defined here as the energy difference between the transition state and a fully assembled reactant complex including the thiyl radical. In order to cope with the large number of conformationally different reactant complexes two limiting cases have been selected here:

(a) the "local reference" case in which the transition state is compared to the preceding reactant complex on the reaction coordinate. In this case transition state and reactant complex share the same hydrogen bonding pattern. This is a realistic description of the situation in a preorganized enzyme active site in which substrate and catalytically active residues can assume only a small number of well defined relative orientations. We will concentrate on this choice of reference in the following discussion.

(b) the "global reference" in which the transition state is compared to the overall most stable reactant complex. This reference is descriptive of a completely unrestricted situation and predicts the reaction barriers under the condition that all components of the reacting system enjoy a maximum of conformational freedom along the reaction coordinate. This choice is certainly not descriptive of the situation in an enzyme active site.

It is important to recognize that both strategies for selection of a reference are still based on stationary points optimized in the absence of a structured surrounding such as an enzyme active site. A realistic description of the latter is only possible by explicit inclusion of all of the active site residues, either in a fully quantum mechanical (QM) model, or in a combined QM/MM model.[24]

In order to separate the effects of the catalytically active residues on the reaction barrier from those on the reaction thermochemistry, we have used eqn. (1) to predict an intrinsic reaction barrier $\Delta E_{C,0}^{\ddagger}$ for the (hypothetical) case of a thermoneutral reaction.[6] True catalysis through external functional groups should lead to a markedly reduced intrinsic barrier while hardly affecting the reaction thermochemistry.

$$\Delta E_C^{\ddagger} = \Delta E_{C,0}^{\ddagger} + 0.5\Delta E_{C,RXN} + \frac{(\Delta E_{C,RXN})^2}{16\Delta E_{C,0}^{\ddagger}} \qquad (1)$$

For the most favorable transition state **17a** in the parent system lacking catalytically active groups the uncatalyzed reaction barrier amounts to +14.7 kcal mol^{-1} with an endothermicity of +8.8 kcal mol^{-1} (Table 1). From these two values, an intrinsic reaction barrier $\Delta E_{C,0}^{\ddagger}$ of +9.8 kcal mol^{-1} can be obtained. The efficiency of acetate catalysis strongly depends on the flexibility of the active site and the possible relative orientations of the glutamate side chain and the ribonucleotide substrate. For the sake of comparison we have overlaid the most relevant part of the RNR X-ray structure reported by Eriksson *et al.*[3] with the optimized transition states in a way that matches the positions of the C2′, C3′, and C4′ ring carbon atoms of the tetrahydrofuran ring as closely as possible (Fig. 2). This projection clearly shows that the side-on orientation of the E441 carboxyl-

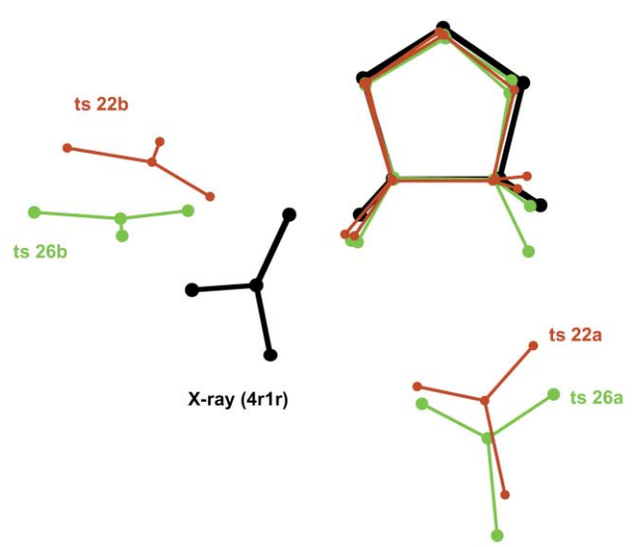

Fig. 2 Overlay of transition states **22a/22b** (red), transition states **26a/26b** (green), and the corresponding substructure of X-ray crystal structure **4r1r** by Eriksson *et al.* (black).[15] The methylthiyl radical has been omitted for clarity.

ate group is much closer, though not identical, to that found in side-on transition states **22b** and **26b**. Comparison of the reaction barriers calculated for these last two transition states with that predicted for the parent system thus represents the most consistent approach for the prediction of hydrogen-bonding effects on the RNR-catalyzed C–H bond activation step. The lowest barrier is predicted for the acetate catalyzed reaction through transition state **22b** at +10.5 kcal mol^{-1}, 4.2 kcal mol^{-1} less than in the parent system. The reaction barrier for the acetamide-catalyzed reaction through transition state **26b** is, however, not significantly larger at +11.2 kcal mol^{-1}, 3.5 kcal mol^{-1} less than in the parent system. Under the condition that we restrict our comparison to side-on complexes only, we arrive at the unexpected conclusion that the catalytic efficiencies of the acetate and acetamide groups are hardly different. Under the additional condition that the side-on complexes optmized here reflect the situation in the RNR active site one would conclude that the experimentally observed differences between the wild type enzyme and the E441Q mutant have to be attributed to changes in later steps of the reaction sequence outlined in Scheme 1.

A different result is obtained when the more stable bridged systems are also considered. Reaction through acetate-bridged transition state **22a** has the lowest overall reaction barrier of +8.2 kcal mol^{-1}, 6.5 kcal mol^{-1} less than in the uncatalyzed system and 2.3 kcal mol^{-1} lower than in the corresponding side-on complex (Table 1). The acetate-catalyzed reaction thus profits strongly from the possibility of forming a bridged reactant complex. The acetamide-catalyzed reaction, in contrast, does not profit from reaction through a bridged complex as the reaction barrier for this pathways is significantly higher than that for the side-on complex. Even though the bridged complexes appear hardly relevant for the RNR-catalyzed reaction due to the well-defined active site, this cannot be assumed to be the case for model systems studied in homogeneous solution.[4,23]

On a more general note the effects of hydrogen bonding on the reaction barrier of a seemingly stereotypical homolytic process identified in this study further supports the hypothesis that enzymatic radical reactions are guided through the active site hydrogen bonding network.[11]

Acknowledgements

This research was supported by the Deutsche Forschungsgemeinschaft and the Fonds der Chemischen Industrie. The calculations described in this study have, in part, be performed on computers of the Leibniz-Rechenzentrum München.

References

1 (*a*) J. Stubbe, *J. Biol. Chem.*, 1990, **265**, 5329; (*b*) J. Stubbe and W. A. van der Donk, *Chem. Biol.*, 1995, **2**, 793–801; (*c*) B.-M. Sjöberg, *Struct. Bonding*, 1997, **88**, 139; (*d*) J. Stubbe and W. A. van der Donk, *Chem. Rev.*, 1998, **98**, 705.
2 S. S. Mao, G. X. Yu, D. Chalfoun and J. Stubbe, *Biochemistry*, 1992, **31**, 9752.
3 M. Eriksson, U. Uhlin, S. Ramaswamy, M. Ekberg, K. Regnström, B.-M. Sjöberg and H. Eklund, *Structure*, 1997, **5**, 1077.
4 R. Lenz and B. Giese, *J. Am. Chem. Soc.*, 1997, **119**, 2784.
5 The water elimination step is also influenced by the neighboring asparagine residue N437: A. Kasrayan, A. L. Persson, M. Sahlin and B.-M. Sjöberg, *J. Biol. Chem.*, 2002, **277**, 5749.
6 M. Mohr and H. Zipse, *Chem. Eur. J.*, 1999, **5**, 3046.
7 P. E. M. Siegbahn, *J. Am. Chem. Soc.*, 1998, **120**, 8417.
8 (*a*) A. L. Persson, M. Eriksson, B. Katterle, S. Pötsch, M. Sahlin and B.-M. Sjöberg, *J. Biol. Chem.*, 1997, **272**, 31533; (*b*) A. L. Persson, M. Sahlin and B.-M. Sjöberg, *J. Biol. Chem.*, 1998, **273**, 31016.
9 C. C. Lawrence, M. Bennati, H. V. Obias, G. Bar, R. G. Griffin and J. Stubbe, *Proc. Natl. Acad. Sci. USA*, 1999, **96**, 8979.
10 F. Himo and P. E. M. Siegbahn, *J. Phys. Chem. B*, 2000, **104**, 7502.
11 (*a*) D. M. Smith, B. T. Golding and L. Radom, *J. Am. Chem. Soc.*, 1999, **121**, 5700; (*b*) D. M. Smith, B. T. Golding and L. Radom, *J. Am. Chem. Soc.*, 1999, **121**, 9388; (*c*) S. D. Wetmore, D. M. Smith, B. T. Golding and L. Radom, *J. Am. Chem. Soc.*, 2001, **123**, 7963; (*d*) D. M. Smith, B. T. Golding and L. Radom, *J. Am. Chem. Soc.*, 2001, **123**, 1664.
12 N. Godbout, D. R. Salahub, J. Andzelm and E. Wimmer, *Can. J. Chem.*, 1992, **70**, 560.
13 (*a*) A. D. Becke, *J. Chem. Phys.*, 1993, **98**, 5648; (*b*) C. Lee, W. Yang and R. G. Parr, *Phys. Rev. B*, 1988, **37**, 785.
14 A. D. Becke, *J. Chem. Phys.*, 1993, **98**, 1372.
15 A comparison of population analysis schemes for DFT calculations on open shell systems has been performed in H. Zipse and M. Bootz, *J. Chem. Soc. Perkin Trans. 2*, 2001, 1566.
16 All calculations have been performed with M. J. Frisch, G. W. Trucks, H. B. Schlegel, G. E. Scuseria, M. A. Robb, J. R. Cheeseman, V. G. Zakrzewski, J. A. Montgomery, Jr., R. E. Stratmann, J. C. Burant, S. Dapprich, J. M. Millam, A. D. Daniels, K. N. Kudin, M. C. Strain, O. Farkas, J. Tomasi, V. Barone, M. Cossi, R. Cammi, B. Mennucci, C. Pomelli, C. Adamo, S. Clifford, J. Ochterski, G. A. Petersson, P. Y. Ayala, Q. Cui, K. Morokuma, D. K. Malick, A. D. Rabuck, K. Raghavachari, J. B. Foresman, J. Cioslowski, J. V. Ortiz, B. B. Stefanov, G. Liu, A. Liashenko, P. Piskorz, I. Komaromi, R. Gomperts, R. L. Martin, D. J. Fox, T. Keith, M. A. Al-Laham, C. Y. Peng, A. Nanayakkara, C. Gonzalez, M. Challacombe, P. M. W. Gill, B. G. Johnson, W. Chen, M. W. Wong, J. L. Andres, M. Head-Gordon, E. S. Replogle and J. A. Pople, GAUSSIAN 98 (Revision A.6), Gaussian, Inc., Pittsburgh, PA, 1998.
17 (*a*) P. E. M. Siegbahn, L. Eriksson, F. Himo and M. Pavlov, *J. Phys. Chem. B*, 1998, **102**, 10622; (*b*) L. A. Eriksson, *J. Am. Chem. Soc.*, 1998, **120**, 8051.
18 (*a*) M. Mohr, H. Zipse, D. Marx and M. Parrinello, *J. Phys. Chem. A*, 1997, **101**, 8942; (*b*) M. Mohr, D. Marx, M. Parrinello and H. Zipse, *Eur. J.*, 2000, **21**, 4015.
19 T. Bally and G. N. Sastry, *J. Phys. Chem. A*, 1997, **101**, 7923.
20 Y. Zhang and W. Yang, *J. Chem. Phys.*, 1998, **109**, 2604.
21 (*a*) B. J. Lynch, P. L. Fast, M. Harris and D. G. Truhlar, *J. Phys. Chem. A*, 2000, **104**, 4811; (*b*) B. J. Lynch and D. G. Truhlar, *J. Phys. Chem. A*, 2001, **105**, 2936.
22 J. W. Ochterski, G. A. Petersson and K. B. Wiberg, *J. Am. Chem. Soc.*, 1995, **117**, 11299.
23 (*a*) T. E. Lehmann and A. Berkessel, *J. Org. Chem.*, 1997, **62**, 302; (*b*) M. J. Robins, Z. Guo, M. C. Samano and S. F. Wnuk, *J. Am. Chem. Soc.*, 1999, **121**, 1425; (*c*) M. J. Robins and G. J. Ewing, *J. Am. Chem. Soc.*, 1999, **121**, 5823; (*d*) T. E. Lehmann, G. Müller and A. Berkessel, *J. Org. Chem.*, 2000, **65**, 2508.
24 (*a*) J. Gao, *Rev. Comp. Chem.*, 1996, **7**, 119; (*b*) K. M. Merz, Jr. and R. V. Stanton, in *Encyclopaedia of Computational Chemistry*, ed. P. v. R. Schleyer, Wiley, Chichester, 1998, pp. 2330–2343; (*c*) J. Tomasi and C. S. Pomelli, in *Encyclopaedia of Computational Chemistry*, ed. P. v. R. Schleyer, Wiley, Chichester, 1998, pp. 2343–2350; (*d*) G. Monard and K. M. Merz, Jr., *Acc. Chem. Res.*, 1999, **32**, 904.